Anchor University Journal of Science and Technology (AUJST)
A publication of the Faculty of Natural, Applied and Health Science, Anchor University Lagos
URL: fnas.aul.edu.ng
In AJOL: https://www.ajol.info/index.php/aujst
Vol. 4 No 2, September 2023, Pp. 233—248
ISSN: 2736-0059 (Print); 2736-0067 (Online)

PRELIMINARY ASSESSEMENT OF AKEREBIATA CLAY DEPOSIT, ILORIN SOUTH WESTERN NIGERIA

[1]J.A. OLATUNJI, [2]O.V. OMONONA, [3]O.V. FATOYE [4]A.G. ANIKOH & [5]F.F. IHOGBETEIN

[1]Department of Mineral & Petroleum Resources Engineering Technology, Kwara State Polytechnic, Ilorin. Nigeria
[2]Department of Geology & Geophysics, Alex Ekwueme Federal University, Ndufu Alike Abakaliki Ebonyi State
[3]Department of Earth Sciences, Faculty of Science and Science Edu, Anchor University, Lagos, Lagos State, Nigeria
[4]Department of Mineral & Petroleum Resources Engineering Kogi State Polytechnic, Lokoja, Kogi State, Nigeria.
[5]Department of Metallurgical Engineering Technology, Kwara State Polytechnic, Ilorin, Nigeria

***Corresponding author Email**: olatunjija11@gmail.com

Submitted 13 February, 2023
Accepted 30 July, 2023

Competing Interests.
The authors declare no competing interests.

ABSTRACT

The study focused on the preliminary assessment of Akerebiata clay deposit Ilorin south western Nigeria. The mineralogical and elemental compositions of the clay sample were determined using X ray diffraction (XRD) and X ray refractory fluorescence (XRF) techniques respectively while the probable reserve of the deposit was estimated using vertical electrical sounding (VES) and horizontal electrical profiling (HEP)(dipole-diploe). Interpretation of results from XRD and XRF revealed that Kaolinite is the dominant clay mineral in the deposit while quartz is the dominant silicate mineral and this indicates that the deposit could be of residual origin. Chemical analysis revealed the predominance of SiO_2, Al_2O_3 with values 61.73% and 27.01% respectively, and low CaO, MgO, K_2O and Na_2O indicates that the clay is probably non expansive and with low feldspar content. Results of the VES shows three geo-electric layers which include: topsoil, clay and basement rocks. The average thickness of the clay layer is inferred to be 6.87m while the area of the deposit is calculated to 42,416.873m^2. With a specific gravity of 2.70, the inferred reserve of the deposit is 781,048tons. These results will be of utmost importance to stakeholders and explorationists in the solid mineral sector.

Keywords: Horizontal Profiling, Akerebiata, Resistivity, Clay, Geochemical

1. INTRODUCTION

The importance of natural resources to national development cannot be underestimated. Nigeria as a nation, unarguably is endowed with numerous natural resources of which clay is one. Understanding the mineralogical, elemental compositional characteristics and obtainable probable reserve has been a daunting exercise in the geosciences community due to low technological know-how, inadequate data and lack of synergetic approach to this study. Sequel to this, is the fact that clay has a lot of industrial applications if adequately explored. This research work sought to address these challenges. Clay is formed either as a product of the chemical weathering of pre-existing granitic rocks and feldspar minerals, particularly in warm tropical and subtropical regions of the world or as a result of the hydrothermal alteration of granitic rocks (Akhirevbulu, *et al.,* 2010). Depending on the amount of water mixed into them, clays exhibit a variety of properties, including plasticity, fluidity, and colloidal and thixotropic properties. These various properties affect industrial and engineering use of clay minerals (Yasin, 2015).

https://dx.doi.org/10.4314/aujst.v4i2.10

According to their mineralogical, clay is a natural fine-grained material that acquires plasticity on being mixed with a limited quantity of water (Aliyu *et al.,* 2012; Shuaib-Babata, *et al.,* 2019). Clays and clay minerals are economic minerals that have been found useful in manufacturing and environmental industries where they serve as major raw materials in the making of ceramic, paint, paper, refractory, plaster of paris and pharmaceutical products (Ojo, *et al.,* 2014). The electrical resistivity method is commonly used in engineering site investigations. It is useful in structural mapping, determination of depth to bedrock, nature of superficial deposits and mineral exploration deposits (Zhody *et. al.* 1974). Afolabi *et. al.* (2013) used the method to investigate the reserve estimate of kaolin deposit and the excavable overburden of the deposits. Egbai (2011) used the vertical electrical sounding (VES) method to study kaolin deposit in Ozanogogo area, Ika South Local Government area, Delta State. Akintorinwa *et. al.* (2012) used vertical electrical sounding technique of electrical resistivity method to determine the geo-electric reserve estimate of laterite deposits along Oshogbo-Iwo highway, southwest Nigeria, a basement complex environment.

2. Location of the Study Area

Akerebiata the study area is located in Ilorin West local Government of parts of Ilorin metropolis (Figure 1). It is situated between longitudes $4^{0}32^{'}$- $4^{0}35^{'}$''E and latitudes $8^{0}30$'-$8^{0}31$N. The area covered is about 42,416.873m^{2}. Weather condition in the region is of two broad types (i.e. rain season and dry season. Annual average rainfall of 1,200mm. The humidity ranges between 60 % and 89%. Mean annual temperature is between 27^{0}C and 30°C. The area is well drained by various streams and their tributaries. The tributaries show dendritic drainage pattern (Ojo *et al.,* 2014: 2017; Olatunji, *et al.,* 2020).

3. Geological Setting

Ilorin is located geographically in the North-Central Nigeria and the rocks belong to the Southwest Basement Complex of Nigeria. The crystalline basement rocks of Ilorin Sheet form part of the West African Craton and the geology closely compares with that of the rest of the basement rocks of Southwestern Nigeria which has been well discussed (Oyawoye, 1972, Rahaman, 1988, Rahaman, 1989, Oluyide *et al.,* 1988). They comprise of migmatite complex of Eburnean age (2000±200ma). Large scale magmatic activities in the area lead to emplacement of Older Granite series of Pan African age. Apart from the isolated hills (particularly the Sobi Hills), most part of the study area is covered by dark sandy or clayey loamy top soils. This is usually followed by laterites which may be as thick as 2m in places. The underlying lithologies consist of weathered to fresh crystalline basement rocks. Main crystalline rocks include; biotite hornblende gneiss with intercalated amphibolites, porphyritic granites and granite gneiss (Figure 3) (Ojo, *et al.,* 2014).

4. Materials and Methods

This study comprises of vertical electrical Sounding (VES), horizontal electrical profiling (HEP) using dipole-dipole method of array and geochemical assessment of the clay deposit.

https://dx.doi.org/10.4314/aujst.v4i2.10

Figure 1: Geographical Map of Nigeria indicating Kwara State (Ajadi, *et al* 2016)

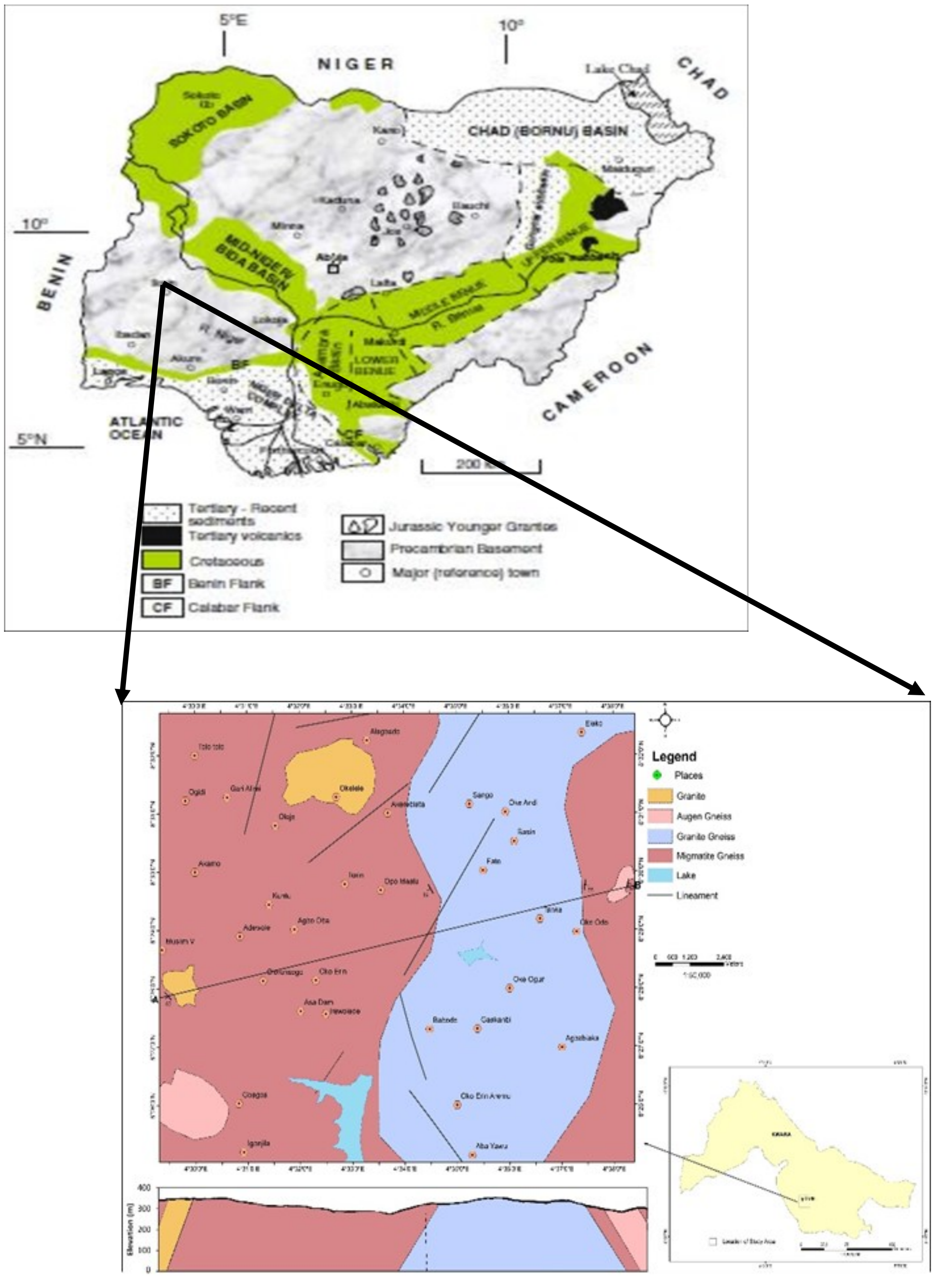

Figure 2: Geological Map of Nigeria and Ilorin showing the Study area (modified after Obaje 2004, NGSA 2007, Olatunji *et al.,* 2020)

https://dx.doi.org/10.4314/aujst.v4i2.10

4.1 Vertical Electrical Resistivity Sounding

The geo-electric sounding data were acquired using Schlumberger array technique and a total of 20 VES stations were conducted across the study area. In vertical electrical sounding (VES), the potential electrodes remain fixed while the current-electrodes spacing is expanded symmetrically about the centre of the spread (Figure 3). The current electrode spread (AB/2) extended to 50m. Herojat Digital resistivity equipment was used which has the capacity to automatically determine the resistance R, such that the three values (Current, I; Potential difference, ΔV and Resistance, R) are displayed after each measurement. The acquired VES data were plotted manually using curve matching and computer iteration. The curves were interpreted qualitatively and quantitatively. The quantitative interpretation was done using partial curve matching technique and the resultant geo-electric parameters were further refined using computer iteration algorithm (IPI2win). The Vertical Electrical Soundings results were presented as sounding curves, geo-electric sections and maps. For geochemical compositional study, two fresh insitu samples were collected at different location within the study area.

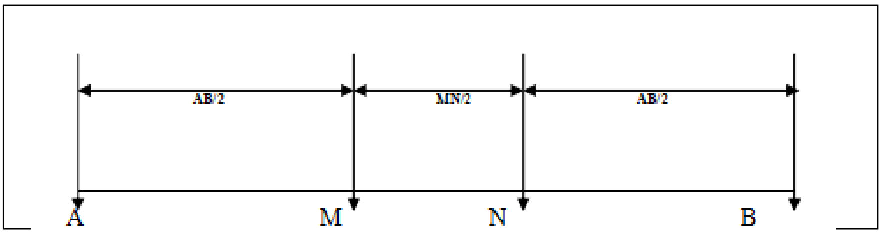

Figure 3: Electrode layout of Schlumberger configuration

Where apparent resistivity, ρ_a is given as:

$$\rho_a = \frac{\left(\frac{AB}{2}\right)^2 - \left(\frac{MN}{2}\right)^2 \times \pi}{2\left(\frac{MN}{2}\right)} \times R \qquad (1)$$

In this array, the pair of current electrodes (A, B) and potential electrodes (M, N) are positioned side by side on the same line (Figure 4). Each pair having a constant mutual separation "a" and "na" is the spacing between the two innermost electrodes (B, M). This array has another factor marked as "n" (the expansion factor). For surveys with this array, the "a" spacing is initially kept fixed, and the "n" factor is increased from 1 - 8 to increase the depth of

https://dx.doi.org/10.4314/aujst.v4i2.10

2D electrical resistivity tomography surveys using Dipole Dipole Array was conducted along Six profile lines across the studied area. The electrical resistivity tomography was obtained using 4m electrode spacing of dipole-dipole configuration. The dipole-dipole spacing enabled the possible detection of subsurface lithology till 50m depth which could be considered satisfactory for the required information about the geological sequence within the study area. The geo-electrical data collected have been processed by means of the *res2DINV* modeling software in order to perform 2D geo -electrical data inversion. The inversion routines are based on the smoothness-constrained least squares method and the forward resistivity calculations were executed by applying an iterative algorithm based on a finite element method. The inversion program divides the subsurface into a number of small rectangular prisms and attempts to determine the resistivity values of the model prisms directing toward minimizing the difference between the calculated and the observed apparent resistivity values. The quality of the fit is expressed in terms of the RMS error. The results obtained from the processing/presentation of field data are presented as 2D resistivity structures, pseudo-sections, and theoretical pseudo-sections (figure 11-13) from which the relevance of this result used in imaging the subsurface by showing different lithologies with respect to their depths of occurrence.

Where the geometric factor (K) is:

$$K= na(n+1)(n+2)\prod \qquad (2)$$ and

Apparent resistivity in Ohm-meter is

$$\rho_a = R*K \qquad (3)$$

Where "R" is Resistance in ohms

The specific gravity of the clay was determined in the laboratory using the relation: $G= M_2-M_1/(M_2-M_1)- (M_3-M_4)$, where M_1=mass of empty Pycnometer, M_2=mass of the Pycnometer with dry soil M_3= Mass of the Pycnometer, soil and water, M4 =mass of Pycnometer filled with water only. The volume of the reserve (m^3) was calculated by finding the product of length, breath and thickness of the deposit. Having taking the coordinate of the boundary, its area was determined using UTM-Geomap software. The thickness of the clay was inferred as showing in Table 3.

4.2. Geochemical Studies

4.2.1 X-Ray Diffraction

The samples of clay collected were analysed using X-ray diffraction spectrometer (XDS 2400H X-ray diffractometer equipped with a MiniFlex2$^+$ goniometer and detector). The samples were oven-dried at 105^{0}C, crushed, milled and homogenized to powders of below 63 µm particle size. About 2g of each sample was placed on XRD's acrylic holder in readiness for analysis. Using XRD equipment ((XDS 2400H X-ray diffractometer equipped with a MiniFlex2$^+$ goniometer and detector).) at CuK" radiation (λ=1.541838Å), 30 mA, 40 kV and 22 reflections, the samples were analysed at 0-90^{0}C every 2 sec count time and 0.02^0 step size. The materials to be analysed were finely ground and sieved to pass through

https://dx.doi.org/10.4314/aujst.v4i2.10

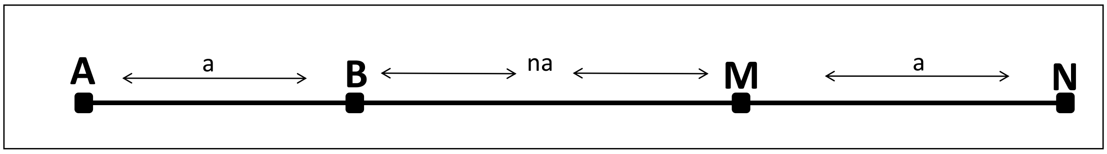

Figure 4: Dipole-dipole configuration

63microns sieve. The pulverized sample was then prepared using prepared blocks and compressed into a flat sample that was later mounted on the sample stage in the XRD cabinet. The sample was analysed using the Emission Transmission spinner stage with the theta-theta settings. The intensity of diffracted X-ray was continuously recorded as the sample and detector rotated through their respective angles. Peak intensities occurred when the mineral containing lattice plane with d-spacing appropriate to different x-rays at a value of θ. passed through the detector.

4.2.2 X-Ray Florescence

The samples were grounded to a fine powder (to obtain a homogenous sample) using a vibration grinding mill with a steel milling. They were sieved through a 200-mesh sieve and dried to constant weight in a furnace at 110 °C. The powder samples were further sub-sampled for particle size determination, XRF, and XRD. XRF was performed on samples prepared in the form of glass disks with a sample/melt ratio of 0.5/5; Li_2B4O_7 was used as the melt. The reference materials GSS8 and BCS-CRM 354 were used to produce standards; mixtures of these with an oxide content including that of the samples to be analysed were used to produce a calibration curve. The reference materials were mixed with a 5% Au/Pt ZGS glass rod and melted in a furnace at a temperature of 1100 °C for 15 min. The melt was taken from the furnace and stirred after 10 min and then replaced to eliminate bubbles. It was then poured into a Pt/Rh 30-mm diameter mold to form a glass disk, of 30 mm diameter and 9 mm thickness were used for the analyses.

5. Results, Interpretation and Discussion

5.1 Interpretation and Discussion of VES Data.

The electrical resistivity method of geophysical prospecting using VES technique was employed to study the subsurface layers to a depth of 50 m around Akerebiata area of Ilorin metropolis. The raw field data and geo-electric parameters were presented in table 1 and 2. Also, Figure 5-8 show the interpreted geo-electric sounding curves with major characteristic of KH and H types. The geo-electric signatures revealed three (3) to four (4) major geo-electric layers in each station. The major geo-electric sequences that were delineated are: topsoil, clay, weathered rock and basement. The topsoil ranges from clayey to Sandy Clay having resistivity and thickness range of 17 - 96 Ωm and 0.4 - 1.9m respectively. This layer is followed by sequence of purely clayey layer with resistivity and thickness range of 8 - 52Ωm, which extended to an average depth of about 7m underlain this, is a fractured to fresh

https://dx.doi.org/10.4314/aujst.v4i2.10

The blue to yellow zone with resistivity range of <31 - 51Ωm along profile one represent conductive zones which is suspected to be due to the presence of clay layer which extended from depth of about 2m to 13m across the profile. Along profile two, coloured zones indicated severely conductive zones, while red to dip yellow coloured zones shows areas with intermediate resistivity and pitch coloured zones represents resistive zones. The estimated average depth to and thickness of the anomaly (Clay) is presented in Table 3.

Table 1: Raw VES Data

AB/2	P1V1	P1V2	P2V1	P2V2	P3V1	P3V2	P4V1	P4V2	P5V1	P5V2
1	81.47	67.58	70.9	31.81	47.36	38.10	68.40	29.95	29.95	29.95
2	48.47	53.75	58.13	28.27	39.52	39.52	54.4	35.67	35.67	35.67
3	32.59	42.75	42.75	25.3	32.59	34.68	43.0	35.25	35.25	35.25
4	28.72	36.99	32.99	22.84	27.2	26.35	34.2	32.99	32.99	32.99
5	30.13	34.62	27.04	20.99	24.7	28.11	28.37	29.95	29.95	29.95
7	35.25	35.25	22.29	19.29	22.7	22.8	21.5	25.21	25.21	25.21
10	43.0	37.89	22.56	19.52	23.39	30.2	22.29	24.55	24.55	24.55
13	49.1	42.1	24.85	20.61	26.71	33.7	25.75	25.92	25.92	25.92
15	52.7	45.13	26.55	21.37	28.37	27.11	28.337	27.71	27.71	27.71
20	58.13	52.47	29.77	23.39	33.39	33.39	36.55	32.59	32.59	32.59
25	62.12	59.55	33.39	26.23	28.37	28.37	44.43	36.55	36.55	36.55
30	64.79	64.79	36.33	29.06	40.73	42.33	53.11	40.49	40.49	40.49
40	69.75	73.54	40.94	32.79	46.51	49.26	70.07	46.51	46.51	46.51
50	75.1	80.1	51.09	41.66	55.1	61.32	81.17	49.20	49.20	49.20

https://dx.doi.org/10.4314/aujst.v4i2.10

Table 2: Geo-electric Parameter of VES Data

Profile	VES Station	Layer	Resistivity (Ωm)	Layer thickness (m)	Depth (m)	Curve type	Infer Lithology
1	VES 1	1	96.9	0.83	0.83	H	Topsoil
		2	18.4	2.29	3.12		Clay
		3	79	--	--		Basement
	VES 2	1	72.7	1	1	H	Topsoil
		2	29.7	6.58	7.58		Clay
		3	105	--	--		Basement
	VES 1	1	74.3	1.4	1.4	H	Topsoil
		2	17.3	6.49	7.88		Clay
		3	55.4	--	--		Basement
	VES 2	1	32	1.39	1.39	H	Clayey Topsoil
		2	17.3	10.2	11.6		Clay
		3	55.4	--	--		Basement
3		1	31.8	1.34	1.34	H	Clayey Topsoil
		2	8.88	1.99	3.34		Clay
		3	90.9	--	--		Basement
	VES 2	1	48.4	1.34	1.34	H	Clayey Topsoil
		2	18.2	6.45	7.79		Clay
		3	68.1	--	--		Basement
4	VES 1	1	23.5	0.5	0.5	KH	Clayey Topsoil
		2	52	1.39	1.89		Clay
		3	15.1	5.28	7.18		Clay
		4	70.5	--	--		Basement
	VES 2	1	68.4	1.52	1.52	H	Topsoil
		2	16.4	8.76	10.3		Clay
		3	4640	--	--		Basement
5		1	23.5	0.5	0.5	KH	Clayey Topsoil
		2	52	1.39	1.89		Clay
		3	15.1	5.28	7.18		Clay
		4	70.5	--	--		Basement
	VES 2	1	23.5	0.71	0.71	KH	Clayey Topsoil
		2	52	1.18	1.89		Clay
		3	8.77	2.75	4.64		Clay
		4	104	--	--		Basement
6	VES 1	1	17	0.5	0.5	KH	Clayey Topsoil
		2	50.1	1.39	1.89		Clay
		3	26.4	5.28	7.17		Clay
		4	148	--	--		Basement
	VES 2	1	20.4	1.98	1.98	H	Clayey Topsoil
		2	31.9	6.88	8.86		Clay
		3	6014	--	--		Basement

https://dx.doi.org/10.4314/aujst.v4i2.10

Table 3: Anomaly Parameter

Profile	VES	Depth to Clay	Clay Thickness
1	1	0.83	2.29
	2	1.0	6.58
2	1	1.4	6.49
	2	0	11.6
3	1	0	3.34
	2	0	7.79
4	1	0	7.18
	2	1.5	8.76
5	1	0	7.18
	2	0	4.64
6	1	0	7.17
	2	0	8.86
Average		0.39	6.82

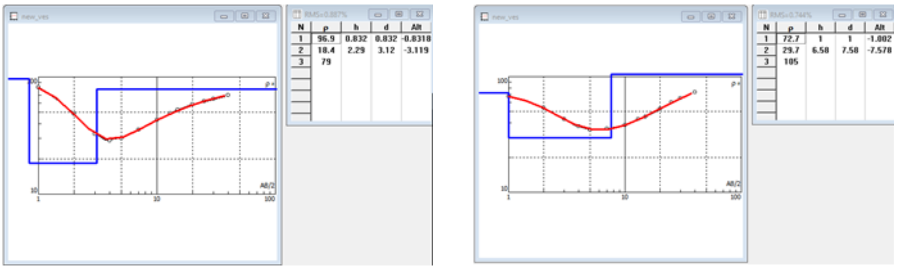

Figure 5: Typical field curve for Profile 1 VES 1 & 2

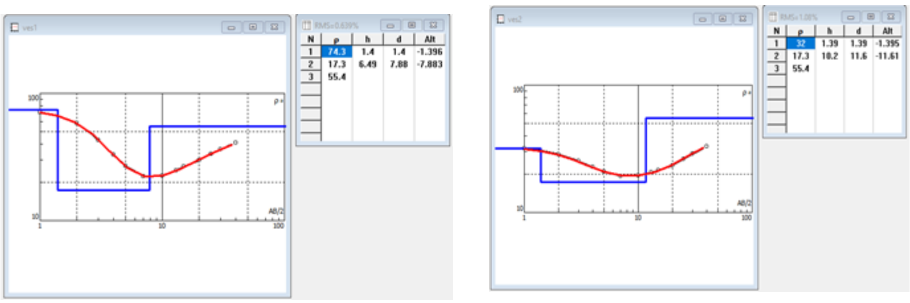

Figure 6: Typical field curve for Profile 2 VES 1 & 2

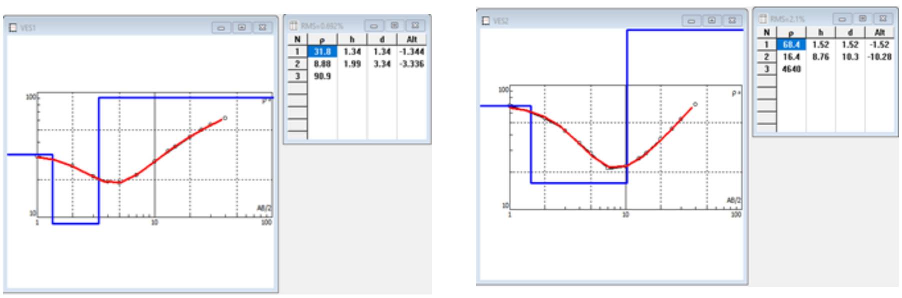

Figure 7: Typical field curve for Profile 4 VES 1 & 2

https://dx.doi.org/10.4314/aujst.v4i2.10

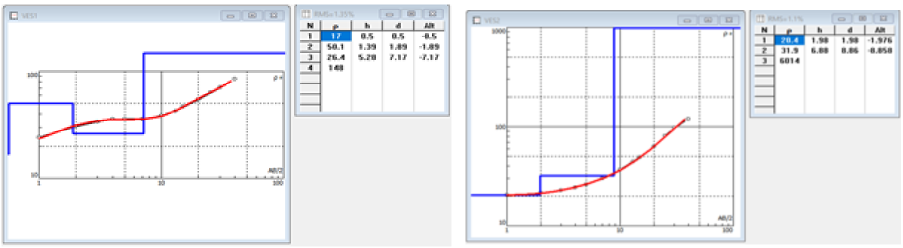

Figure 8: Typical field curve for Profile 5 VES 1 & 2

5.2 Interpretation and Discussion of Horizontal Electrical Profiling.

The 2D resistivity structure along traverse one (figure 11a) shows a thick conductive rock buried beneath stations around the distance of 10m to 70m, which extended to 10m depth, and suspected to be an unconsolidated materials ranging from topsoil to weathered layer. Also, conductive zones are seen towards the two extreme ends of the profile from depth range of 15 to 25m down to the base, this is suspected to be fractured basement rock layer. The resistive zones are seen around the distance of 0 to 10m and 70m to 100m towards the surface which extended to the depth of 20m and infinitely sandwiched by conductive zones from distance of 25m to 75m. The resistive zones might be as a result of competency of some parts of the basement rock. The second traverse (figure 11b) also shows a predominantly conductive area towards the surface from distance of 20m till end of profile which extended to the depth of about 10m from the distance of 20m to 50m and thinner till the end of the profile. This zone which is suspected to be the unconsolidated zone with pockets and flanks of conductive structures present at various points in the pseudo section.

Also, conductive zones are seen towards the two extreme ends of the profile from depth range of 17 to 25m down to the base, this suspected to be fractured basement rock layer. The resistive zones are seen around the distance of 0 to 10 and 65 to 100 towards the surface which extended to the depth of 17m and infinitely sandwiched by conductive zones from distance of 25 m to 75m. These zones might be as a result of presence of competent basement rock. Furthermore, the 2D resistivity structure in the third traverse (figure 12a) depicts a layer of highly conductive structure running from distance 20m to 60m along the profile which extended to about 5m depth across the study area. This traverse is generally more resistive compare to previous traverses that is the slightly resistive layer run from distances 0 to about 20m, 30 to 70m and 70 to 100m to a depth of 15 m, infinite and 20m respectively along the traverse.

In figure 12b (traverse four), a layer of the less resistive structure extends over from distance of 40 to 60m with a shallow depth of less than 5m. The rest of the pseudo-section is filled with more resistive structures with a pocket of slightly conductive structure present towards the beginning (0 to 25m) and the end (80 to 100m) of the traverse starting from a depth of around 15 to 27m to infinity. Therefore, the blue colour zones towards the surface are characteristically weak

https://dx.doi.org/10.4314/aujst.v4i2.10

5.3 Correlations between VES and Dipole-dipole techniques

The geo-electric section (figure 10 and 11) around VES 1, 2 and 4 demonstrated weak zone which also coincides with Dipole – Dipole Pseudo-section (Figure 8) at a distance 20 to 65m. This also agrees with the low resistivity zone observed on the dipole-dipole pseudo-section (figure 8) at a distance 20 to 40m and geo-electric section which indicate low integrity and high susceptibility to failure, if the structure is lay within this zone (VES 1, 2 and 4). Also, VES 3 shows presence of thin layer of an unconsolidated material which correlated with results obtained from traverses three and four. Therefore, Correlating the electrical resistivity methods employed along traverses contributed well in identification of weak zones, these weak zones will contribute a great deal to any structure within this zone. The result shows that clay and clayey sand is more predominant within the study location. These results reveal that the techniques used for this study are complementary.

5.4 Reserve Estimates

The cost of removing the overburden thickness should be considered in mining operation. It is important to take into cognisance the economic viability of the mining. The rock overburden thickness ratios of 1 to 1 very much satisfy the universal profitability factor of thickness ratio of 0.5 for mineral deposits. Though the over-burden materials are not waste as they could be excavated and marketed as 'bulk-fill materials', where their thickness is more than the rock thickness are not considered in order to minimize the cost of removing the overburden, environmental implication and profitability. The calculation of the rock mass: overburden thickness ratios in prospective areas revealed a ratio of 17 to 1, which very much satisfy the universal profitability factor of thickness ratio of 0.5 for mineral deposits.

Reserve Volume (m^3) = Length X Breadth X Thickness

Area = Length X Breadth = 42,416.873 m^2

Considering the average depth of 6.82 m (i.e. the thickness of the clay)

The Volume = Area X Thickness

= 42,416.873 m^2 X 6.82m = 289277.12 m^3

The Specific Gravity = 2.70

Total Tonnage = Volume X Specific Gravity

Hence, Calculated Reserve = 289277.12 X 2.70

= 781,048 tons

5.4 Geochemical Assessment of the Clay Deposit

5.4.1 Interpretation and Discussion of X-ray Diffraction Results.

The result of X-ray diffraction test carried out is presented in Table 4 above. The result revealed the presence of Kaolinite, Quartz, Muscovite, Microcline, Cristobalite, Albite, Halloysite. The Diffractogram obtained from the XRD analysis in the region revealed the dominant clay mineral as kaolinite with minor muscovite. The result revealed quartz and microcline as the most abundant non-clay minerals while kaolinite was found to be the principally dominant clay mineral, other accessory minerals are muscovite, cristobalite, albite, halloysite. Mineral composition of

https://dx.doi.org/10.4314/aujst.v4i2.10

Table 4: Results of X-ray Diffraction.

Peak	2θ/degree	Plane	Intensity	d-Valve (A°)	Minerals.	% Composition
1	11.98	2 3 1	13.26	7.3878	Kaolinite	3.81
2	20.64	2 1 1	37.93	4.3032	Quartz	10.89
3	26.50	1 1 2	85.85	3.3635	Quartz	24.64
4	34.50	2 1 3	7.29	2.5996	Kaolinite	2.09
5	36.43	1 1 0	72.91	2.4663	Quartz	20.92
6	42.50	3 1 0	17.95	2.1270	Muscovite	5.15
7	50.14	2 2 1	61.82	1.8193	Microcline	17.74
8	60.20	1 1 4	16.88	1.5372	Cristobalite	4.84
9	68.79	0 0 4	12.75	1.3651	Albite	3.66
10	78.00	3 1 1	21.82	1.2250	Halloysite	6.29

quartz was found to be 56.45% followed by microcline 17.74%, halloysite 6.29%, kaolinite 5.90%, kuscovite 5.15%, cristobalite 4.84% and albite 3.66%. Kaolinite is the dominant clay mineral, this suggest that the environment of formation is a well-drained environment and that the clay has little potential for expansion. Equally, it has low shrinkage potential when subjected to drying. (Adeyemi *et al,* 2003).

Quartz was identified in the sample indicating that it is the dominant mineral in the clay deposits in the study area. Its high dominance clearly explained its grittiness and suggests that the clays could be of residual origin (Akhirevbulu *et al.,* 2010). Kaolinite was found to be the dominant clay mineral. The non-clay minerals include quartz, anatase, rutile, plagioclase and microcline. High silica contents with low alumina, and less alkali, revealed by the chemical characteristics signify Kaolinitic features. The mineralogical assemblage of the clay therefore suggests an extent of kaolinitization. Presence of feldspar in the sample suggests an incomplete alteration and formation of the clay from in situ weathering of the older crystalline rocks in the study area (Ekosse, and Ngole, 2012).

5.4.2. Interpretation and Discussion of X-ray Florescence results.

The result of X-ray florescence (XRF) is presented in Table 5 above, the result revealed that the major element of the clay deposit is dominated by SiO_2, Al_2O_3 and Fe_2O_3 with a composition of 61.73%, 27.01% and 3.91% respectively. Other oxides found

https://dx.doi.org/10.4314/aujst.v4i2.10

Table 5: Results of X-ray Florescence

S/N	Basic Oxides	Formulae	% Composition
1	Silicon Oxide	SiO_2	61.73
2	Aluminum Oxide	Al_2O_3	27.01
3	Lead Oxide	PbO	0.01
4	Calcium Oxide	CaO	0.36
5	Iron Oxide	Fe_2O_3	3.91
6	Magnesium Oxide	MgO	1.35
7	Potassium Oxide	K_2O	1.50
8	Chromium Oxide	Cr_2O_3	0.06
9	Sodium Oxide	Na_2O	1.74
10	Phosphorus Oxide	P_2O_5	0.12
11	Sulphide	SO_3	0.05
12	Manganese Oxide	MnO	0.01
13	Titanium Oxide	TiO_2	0.40
14	Barium Oxide	BaO	0.09
15	Copper Oxide	CuO	0.01
16	Loss of Ignition	LOI	1.28

are Na_2O, K_2O, MgO, TiO_2, P_2O_5, CaO, BaO, Cr_2O_3, SO_3, CuO, MnO and PbO with the composition 1.74%, 1.50%, 1.35%, 0.40%, 0.12%, 0.36%, 0.09%, 0.06%, 0.05%, 0.01%, 0.01%, 0.01% respectively. The ratio of SiO_2/Al_2O_3 ranging from 1.69 to 3.86 implies presence of siliceous sands and this can be attributed to high quartz content. Moore *et al.,* (1989), have proposed that quartz (SiO_2) may occur as fine disseminated crystalline particles in kaolinite or deposited with tiny flasks of the clay minerals, so, the mean values of SiO_2 content of the clays which is in excess of 50% implies that quartz is the main constituent of the clay samples. The relatively high percentage of alumina (Al_2O_3) is probably related to the clay minerals and feldspar in the deposit. The relatively low Fe_2O_3 may be responsible for non-detection of iron oxide minerals haematite or goethite from the XRD analysis of the clays. Low CaO, MgO, K_2O and Na_2O suggest the clays are most probably non expandable/ swelling and low feldspar content. According to (Millot, 1970), the composition suggests that the clay samples are hydrated siliceous aluminosilicates. The LOI which is a measure of organic matter content and other combustible fractions, chemically combined water and CO_2 have mean percentage of 1.28%. This low-moderate value could be attributed to the absence of carbonates rock. In addition, according to Payne (1961) cited in Osabor *et al.,* (2009), the obviously high content of Al_2O_3 combined with SiO_2 (Al_2O_3 + SiO_2 = 88.74%) indicates that the clay is good for paint manufacturing. Also, with respect to SiO_2/ Al_2O_3 ratio, which exceeds the recommended minimum of 2:1 Worall (1975), the clay is deemed usable for refractory works. In the view of Osabor et al (2009), the low content of fluxing and ion exchange materials, that is, Na, K and Mg is indicative of Low fluxing and ion exchange potentials of the clay. The CaO is found to be low and this makes the clay good for ceramics. High content of CaO may lead to expansion and subsequent cracking structures (Obaje and Ekpenyong, 1997).

6. Conclusions

The preliminary assessment of Akerebiata clay deposit South-western Nigeria has been examined in this study. This is considered necessary in order to ascertain its economic potential quantitatively and qualitatively. Twenty vertical electrical sounding and horizontal electrical profiling along six profiles were conducted while the mineralogical and chemical compositions were determined using XRD and XRF. Results of the VES shows three to four geo-electric layers which include: topsoil, clay, weathered rock and basement rocks. The average thickness of the clay deposit was inferred to be 6.87m while the area of the deposit is calculated to 42,416.873m^2. With a specific gravity of 2.70, the inferred reserve of the deposit is 781,048tons. The clay mineral is dominated by Kaolinite clay mineral, this suggest that the environment of formation is a well-drained environment and that the clay has little potential for expansion. Equally, it has low shrinkage potential when subjected to drying. The outcome of this study will be of utmost importance to the stakeholders and explorationists in the solid mineral sector.

References

Adeyemi, G. O., Olarewaju, O. B., Akintunde, O.B. and Mesida, O. T. (2003): Mineralogical and Geotechnical Characteristics of some Subgrade Soils in a Section of the Ibadan /Ile- Ife Express Way, Southwestern Nigeria. Journal of Applied Sciences, 6 (2): Pp3536 - 3547

Afolabi, O, Olorunfemi, M.O, Olagunju, A.O and Afolayan J.F. (2004). Resource quantification of kaolin deposit using the electrical resistivity method - Case study from Ikere-Ekiti, Southwest Nigeria. Ife Journal of Science Vol. 6, No: 1, Pp. 35-40.

Ajadi, B.S., Adaramola, M.A., Adeniyi, A., and Abubabkar, M.I. (2016). Effect of Effluents Discharge on Public Health in Ilorin Metropolis, Nigeria. Ethiopian Journal of Environmental Studies & Management 9(4): Pp389 – 404.

Akhirevbulu O.E. Amadasun C.V.O., Ogunbajo M.I. and Ujuanbi O. (2010). The Geology and Mineralogy of Clay Occurrences Around Kutigi Central Bida Basin, Nigeria. Ethiopian Journal of Environmental Studies and Management Vol.3 No.3. Pp49-56. 3(6):Pp 62-67

Akintorinwa, O. J., Ojo J. S. and Olorunfemi M. O. (2012). Geo-electric Reserve

https://dx.doi.org/10.4314/aujst.v4i2.10

Estimation of laterite deposit along a basement complex underlain Osogbo- Iwo Highway Southwest Nigeria. The Pacific Journal of Science and Technology Vol. 13, Pp 490 – 496

Aliyu, S., Garba, B., Danshehu, B. G., Argungu, G. M., and Isah A. D. (2014). Physio-Chemical Analysis of Gwarmi Clay Deposit, Wurno Local Government Area of Sokoto State, Nigeria, The International Journal of Engineering and Science (IJES), (IJES), 3(6):Pp 62-67

Egbai, J.C. (2011). Vertical Electrical Sounding for the investigation of kaolin deposits in Ozanogogo Area of Ika South Local Government Area of Delta State, Nigeria. Journal of Emerging Trends in Engineering and Applied Sciences (JETEAS) 2(1): Pp147-151

Ivana. S., Stanisa, S., Ivan., S and Dragoljub G. (2014). Industrial Application of Clays and Clay Minerals. Nova Science Publishers, Inc.New York. Pp.379-402

Millot, G. (1970). Geology of Clays: Weathering in Sedimentology.– Geochemistry; Springer, Heidelberg-Berlin – Masson, Paris – Chapman and Hall, London Pp 429.

Obaje, N., H. Wehner,G. Scheeder, K. Abubakar and A. Jauro, (2004). Hydrocar-bon Prospectivity of Nigeria's Inland Basins. From the viewpoint of Organic Geochemistry and Organic Petrology AAPG Bulletin 88(3):Pp325-353

Ojo, O.J. Adepoju, A.S.,and Alhassan, N. (2014). Geochemical and Mineralogical Studies of Kaolinitic Clays in Parts of Ilorin, Southwestern Basement Rock Area, Nigeria Universal Journal of Geoscience 2 (7): Pp212-221.

Ojo, O.J. Egbanubi, O.E. Adepoju, S.A. Adeoye, M.O. Adedoyin, A.A. and Sola-Ojo, F.E. (2017). Evaluation of Chemical Composition and Mineralogical Characteristics of Clays in Some Part of Kwara State: Implications for Geophagy. Proceedings of The 2016 Faculty of Science International Conference Pp 80-82.

Olatunji, J.A., Olasehinde, D.A., Olsehinde, P .I., Awojobi, M.O., Akinrinmade, O.A. and Obaro, R.I. (2020). Preliminary Integrated Assessment of Hydrogeological Conditions, a case study of Parts of Ilorin Crystalline Rocks South-western Nigeria. Journal of Applied Geology and Geophysics. Vol. 8, (5) Pp 01-06

Oluyide, P.O., C.S. Nwajide, and A.O. Oni, (1988). The geology of Ilorin area, Bulletin Geological Survey of Nigeria; 42, Pp.60-66.

Osabor, V.N., Okafor, P. C., Ibe, K.A. and Ayi, A.A. (2009): Characterization of clays in Odukpani, South eastern Nigeria. African Journal of Pure and Applied Chemistry Vol. 3 (5), Pp. 079-085

Oyawoye, M.O., (1972). The basement complex of Nigeria In: Dessauvagie TFJ, Whiteman AJ (eds) African geology, Ibadan University Press, (15) Pp. 66–102.

Payne, H.F. (1961): Organic Coating Technology II, Pigments and Coating, (John Wiley and Sons, Inc New York) Vol. (2) Pp 982

Rahaman, M.A., (1988). Recent advances in the study of the Basement Complex of Nigeria. In Precambrian geology of Nigeria, Geo logical survey of Nigeria, Kaduna, Pp11-43

Rahaman, M.A., (1989). Review of basement geology of southwestern Nigeria. In Kogbe, C.A. (Ed.), Geology of Nigeria, 2nd Edition. Rock View (Nigeria) Ltd., Jos, Pp.39-56.

Shuaib-Babata, Y.L., Ambali, I.O., Ibrahim, H.K., Ajao, K.S., Elakhame, Z.U. N. I. Aremu, N.I. and Odeniyi, O.M. (2019). Assessment of Physico-Mechanical Properties of Clay Deposits in Asa Local Government Area of Kwara State Nigeria for Industrial Applications Journal of Re search Information in Civil Engineering, Vol.16, No.2 Pp. 2727-2753

Worall, W.E. (1975): Clay and Ceramic Raw Materials, (Applied Sciences Publications, London). Pp 203.

Yasin, E. (2015). Physiochemical Properties of Handere Clays and Their Uses as a building Material. Journal of Chemistry. Vol (21) Pp 1-6.

Zohdy, A.A.R., Eaton, G.P. and Mabey, D.R. (1974). Application of Surface Geophysics to Ground-Water Investigations, In Techniques of Water-Resources Investiga- tions of the United States Geological Survey. Book 2, Chapter D1. Pp 63.

https://dx.doi.org/10.4314/aujst.v4i2.10